HHS Public Access

Author manuscript

J Orthop Res. Author manuscript; available in PMC 2020 August 01.

Published in final edited form as:

J Orthop Res. 2019 August ; 37(8): 1817–1826. doi:10.1002/jor.24324.

Brown fat promotes muscle growth during regeneration

Anna R. Bryniarski[1], **Gretchen A. Meyer, PhD**[1,2,*]

[1]Departments of Investigation performed at the Program in Physical Therapy, Washington University in St. Louis; St. Louis, MO 63108

[2]Departments of Neurology, Orthopaedic Surgery and Biomedical Engineering, Washington University in St. Louis; St. Louis, MO 63108

Abstract

Accumulation of adipose tissue around and within muscles is highly correlated with reduced strength, functional limitations and poor rehabilitative outcomes. Given the intimate physical contact between these tissues, paracrine cross-talk is a likely mediator of this association. The recent discovery that muscle-associated adipose tissue exhibits features of beige fat has suggested that this cross-talk may be modifiable, as beige fat can be stimulated to assume features of brown fat. In this work, we describe a novel intermuscular fat transplant model in the mouse rotator cuff to investigate cross-talk between muscle and adipose tissue. Specifically, we examine the role of transplanted fat phenotype on muscle regeneration by transplanting pieces of classical brown (interscapular), beige (inguinal) or white (epididymal) adipose tissue in conjunction with cardiotoxin injection to the adjacent supraspinatus muscle. Transplantation of brown fat, but not beige or white, significantly increased muscle mass, fiber cross sectional area and contractile force production compared with sham injury. This effect was not seen when cardiotoxin was delivered to a distant muscle, or when adjacent muscles were injected with saline indicating that the effect is localized and specifically targeting the regenerative process. Thus, we conclude that local signaling between fat and muscle varies by phenotype and that brown fat supports regeneration. Clinical significance: Our findings suggest that the phenotype of muscle-associated fat could be a novel therapeutic target to modulate fat-muscle signaling.

Keywords

Brown Fat; Muscle; Cross-talk; Paracrine Signaling; Regeneration

Introduction

Originally viewed simply as a source of free fatty acids for metabolic processes, adipose tissue is now recognized to secrete a host of bioactive cytokines and chemokines (so called

*Corresponding Author: Dr. Gretchen A.Meyer, 4444 Forest Park Ave, Suite 1101, St. Louis, MO 63108, Tel: 314-286-1456, Fax: 314-747-0674, meyerg@wustl.edu.

Author Contributions Statement: ARB: Acquisition, analysis and interpretation of data, manuscript drafting and revision. GAM: Conceptualization and study design, acquisition, analysis and interpretation of data, manuscript drafting and revision. All authors approve submission of this manuscript.

The authors have no conflicts of interest to disclose.

"adipokines") that impact both local and distant tissues. The type and nature of secreted adipokines is not uniform across the body, but varies by location, or "depot", of adipose tissue[1]. This heterogeneity is important as it permits site-specific regulation of tissue function via paracrine signaling[2;3].

Paracrine cross-talk has been proposed between skeletal muscle and the intimately-associated epimuscular adipose tissue (outside the muscle boundary; EMAT) and intramuscular adipose tissue (within the muscle boundary; IMAT)[4–6]. A number of pieces of evidence support this hypothesis, though conclusions about the nature of the signaling are mixed. In humans, excesses of both EMAT and IMAT develop with age, injury and disease[6;7] and are strongly correlated with declines in muscle strength and responsiveness to rehabilitation (EMAT[8–11], IMAT[12–15], EMAT+IMAT[16–20]). This correlation persists even after accounting for differences in visceral adiposity in obese individuals[10;21], and may be specific to a single muscle or muscle group[15;16]. Taken together, this suggests that EMAT and IMAT locally impair the ability of muscle to generate force and respond to loading. On the other hand, genetic ablation or mutation of IMAT progenitor cells (fibroadipogenic progenitors; FAPs) in mouse muscle impairs regeneration[22;23], leading to the hypothesis that IMAT secretes pro-myogenic cytokines that promote regeneration[22]. These seemingly contradictory conclusions may be reconciled by considering the pathological state of the adipose tissue. That is, it is possible that while EMAT and IMAT play an important physiological role in health, they are altered by pathology causing them to impair rather than support muscle function.

In support of this hypothesis, differences in the characteristics of EMAT and IMAT have been noted with injury and disease. Specifically, our recent work demonstrates that EMAT in the human rotator cuff exhibits transcriptional features of beige fat which are reduced in injured shoulders[24]. Similarly, progenitors isolated from healthy human limb muscle have beige characteristics[25] that are not observed in those from obese individuals[26]. Such phenotypic shifts have significant clinical implications as beige fat can be exogenously stimulated ("browned"), which alters its physiological influence by modifying its secreted adipokine profile[27;28]. As a whole, this evidence suggests that the phenotype of EMAT and IMAT may represent a novel therapeutic target whereby targeted browning could restore physiologically beneficial paracrine signaling. However, the role of adipose phenotype in paracrine fat-muscle cross-talk is difficult to mechanistically explore in existing models. Classical methods of adipose browning (e.g. cold exposure) and genetic modulation of browning are systemic in nature and are thus complicated by endocrine effects from distant depots. Pharmacological compounds, which could be delivered locally to muscle, may directly impact other muscle-resident cells making it difficult to isolate adipose effects.

To address these issues, in this work, we describe the development of a novel intermuscular fat transplant mouse model to study local signaling between adipose tissue and skeletal muscle. This model allows independent control of adipose and muscle biology and can be combined with established disease and genetic models to test mechanistic hypotheses. Here, we use this model to evaluate the role of adipose phenotype on local muscle regeneration and demonstrate that signals from brown, but not beige or white fat, promote muscle growth during regeneration. These findings represent the first in-vivo demonstration of local

signaling between adipose tissue and skeletal muscle and the first evidence that brown fat can promote muscle regeneration.

Methods

Experimental Design.

Experiments were performed on 10 week old male C57BL/6J mice (Jackson Laboratory, Bar Harbor, ME) in standard housing at 22 °C. Mice were divided into four transplant groups by the source of the transplanted fat: “brown” (interscapular), “beige” (inguinal), “white” (epididymal) and “sham” (no transplant). Transplant groups were further divided into two treatment groups: graft-adjacent regeneration and graft-distant regeneration with N=6 mice in each of the 8 groups. Experiments were performed on cohorts of mice comprising 4 co-housed littermates, one in each transplant group and were allocated and assessed in random order. An additional group of 4 mice (fat transplant with graft-adjacent regeneration) were included in the study for the histological assessment of fat engraftment as described below. All muscle measures were recorded by a researcher blinded to experimental grouping. All procedures were performed in accordance with the National Institutes of Health’s Guide for the Use and Care of Laboratory Animals and were approved by the Animal Studies Committee of the Washington University School of Medicine.

Induction of Muscle Regeneration.

Mice were continuously anesthetized with 2% isoflurane at 2 L/min. A small (~2mm) incision was made through the skin over the spine of the scapula to expose the scapular insertions of the deltoid and trapezius muscles (Fig 1A *dotted line*). A second small incision was made through the trapezius muscle at the scapular insertion to open an intermuscular pocket between the trapezius and supraspinatus (SS) muscles (Fig 1B *dotted line*). Then, 10 uL of either 10 μM cardiotoxin (CTX; *naja mossambica mossambica* Sigma Aldrich, St. Louis, MO) or sterile saline (SAL) was injected along the mid-line of the SS muscle through the opening to induce focal muscle regeneration[29]. Mice receiving SAL injections to the SS received CTX injections in the tibialis anterior (TA) muscle without surgical exposure as described previously[30].

Isolation and Transplantation of Fat Grafts.

Fat used for transplantation was isolated from interscapular, inguinal and epididymal fat depots of 3–4 week old C57BL/6J or C57BL/6-Tg(CAG-EGFP) donor mice under anesthesia. The dissection and characterization of these fat depots has been described previously[31]. A 3–4 mg piece of fat was isolated from the appropriate depot, weighed and pushed gently into the intermuscular pocket (Fig 1C). 5–0 braided silk suture was used to secure the trapezius to the deltoid muscle at the incision site and then the skin was closed with Vetbond. Donor mice were euthanized following transplantation procedures and recipient mice were allowed to recover with analgesia (5–10 mg/kg body weight meloxicam) and free cage activity. 2 weeks post-surgery, animals were euthanized and grafts were removed from both shoulders, weighed and combined for gene expression analysis. Also at this time, SS muscles were isolated for ex-vivo contractile mechanics testing and histological analysis. Data from right and left SS muscles were averaged for each mouse. TA

muscles were also harvested at this time in the graft-distant regeneration group, weighed and frozen for histological analysis.

Quantitative PCR.

RNA was extracted from harvested grafts, quantified, reverse transcribed and transcripts detected as described previously[24]. The primer sets for the genes of interest are listed in Supplemenary Table 1. Hierarchical clustering was performed on log10 and gene-normalized data using a custom analysis code using the complete linkage method of the hclust function in R.

Contractile Mechanics Testing.

Details of the SS ex-vivo preparation can be found in Supplemental Figure 1. Briefly, the scapula was dissected free of all musculature except the SS which maintained both its proximal and distal insertions. The proximal aspect of the scapula was secured to a custom lever arm at the proximal scapula. Suture was also knotted at the distal tendon for anchoring to a rigid post. The humeral head was then bisected with surgical scissors to provide a bony anchor to prevent tendon slippage and the glenoid fossa was removed to improve free extension of the tendon. The scapula with attached SS was then transferred to a custom muscle physiology testing system (1500A, Aurora Scientific). The lever arm was secured to a dual mode force transducer/lever system (305C-LR) and the distal suture secured to a rigid post in a bath of Ringer solution (137mM NaCl, 5mM KCl, 1mM NaH_2PO_4, 24mM $NaHCO_3$, 2mM $CaCl_2$, 1mM $MgSO_4$ 11mM glucose, 10 mg/L curare) maintained at 37 °C. The secured muscle was flanked by parallel plate electrodes enabling electrical stimulation.

Peak tetanic force was determined by increasing muscle length incrementally from slack length and eliciting tetanic contraction (300ms pulse, 20V, 225 Hz) until a plateau in force was reached. A twitch contraction was also recorded to enable assessment of twitch kinetics. The fiber length at peak was measured with a flexible ruler and then the muscle was dissected free, weighed and flash frozen in liquid nitrogen cooled isopentane for histological analysis. Peak tetanic stress and peak twitch stress were computed by dividing the respective peak forces by physiological cross-sectional area (PCSA=(muscle mass * cos(pennation angle))/(muscle density * fiber length)), assuming a muscle density of 1.056 g/cm^3 and a pennation angle of 16.92 degrees. Twitch kinetic parameters were calculated from raw force curves as the time between the onset of stimulation and peak force (time to peak tension) and half the time between peak force and complete relaxation (half-relaxation time).

Histological Analysis of Cellular Composition.

Axial sections of frozen SS muscles were cut at the approximate position of fat engraftment. Sections were immunostained against myosin heavy chain (MHC) isoforms (Developmental Studies Hybridoma Bank; BA-F8, SC-71, BF-F3 and 6H1), Pax7 (Developmental Studies Hybridoma Bank; PAX7), PDGFRa (R&D systems; AF1062) and counterstained against laminin (abcam; 11575) and DAPI. 2 20x images were acquired in both the superficial (graft adjacent) and deep (graft distant) regions, yielding at least 200 fibers analyzed per region per muscle. Fiber areas were detected and quantified by a custom macro in ImageJ (NIH; Bethesda, MD) based on the laminin signal. Areas were subdivided by fiber type based on

MHC staining. Satellite cells were identified as Pax7+ nuclei located underneath a laminin+ basal lamina. FAPs were identified as PDGFR+ cells in the interstitial space between laminin+ fibers. Sections of SS and TA muscles were also stained with hematoxylin and eosin (H&E) to confirm penetrance of cardiotoxin into the region of interest, identified by regions with centralized nuclei[30]. Muscles with less than 50% penetrance were excluded from further analysis.

Histological Analysis of Fat Engraftment.

Scapula/SS/graft composites were either flash frozen in liquid nitrogen cooled isopentane or formalin fixed for 48 hours, dehydrated in alcohol and embedded in paraffin. Frozen composites were cut into 10 μm cryosections which were formaldehyde vapor fixed for 48 hours at −20°C. Paraffin embedded composites were cut into 10 μm sections which were then cleared in xylene and subjected to heat-induced antigen retrieval in 0.1 M citric acid (pH 6) at 90°C for 15 minutes. Immunostaining was performed against GFP (Life Technologies; A21311), UCP1 (abcam; ab10983) and perilipin (Progen; GP29). Once fluorescent images were acquired, sections were stained with hematoxylin and eosin (H&E) and re-imaged to provide additional morphological information.

Statistical Analysis.

Gene expression analysis in fat grafts was analyzed by 2-way ANOVA across time and fat type. A Bonferroni post-hoc was used to determine significant comparisons between groups. All muscle comparisons were performed with 1-way ANOVA with cohort-matching and a Tukey post-hoc test to determine significant comparisons between groups. All significance levels (α) were set to 0.05 and all data are presented as means ± standard errors.

Results

Transplanted fat engrafts in the intermuscular space

At 2 weeks post-transplant, recipient mice exhibited no signs of morbidity and grafts of all three fat phenotypes appear vascularized without gross signs of rejection or necrosis. Blood filled vessels are apparent in grafts at harvest during dissection (Fig 2 A–C, arrows) and in hematoxylin and eosin stained sections of harvested grafts (Fig 2 D–E, arrows). Immunostaining grafts for CD68, a marker for circulating and resident macrophages, revealed a diffuse distribution of positive cells amongst perilipin positive adipocytes not indicative of immune rejection. Phenotype-characteristic adipocyte morphology is also maintained in grafts, with brown grafts composed primarily of multilocular adipocytes (Fig 2 D, G), beige grafts composed of a mixture of multilocular and small unilocular adipocytes (Fig 2 E, H) and white grafts composed of large unilocular adipocytes (Fig 2 F, I). Transplanted grafts from GFP expressing mice appeared to remain outside the muscle fascial boundary and no GFP positive cells were detected within the muscle belly (Supplemental Figure 1).

Transplanted fat maintains phenotype-specific characteristics

At the graft-muscle interface, intimate contact between perilipin positive adipocytes (green) and muscle resident cells (adjacent DAPI stained nuclei) is apparent for all fat phenotypes

(Fig 3 A–C, insets). Histological sections of brown grafts also show high concentrations of the brown-adipocyte characteristic protein uncoupling protein 1 (UCP1) compared with beige and white, suggesting a maintenance of phenotype specificity in transplanted fat (Fig 1A). To further explore the maintenance of phenotype specificity, transplanted grafts were transcriptionally profiled by expression of a subset of 8 adipogenic genes spanning brown-selective (Ucp1, Cidea and Eva1), beige-selective (Tmem26, Tnfrsf9/CD137 and Tbx1), white-selective (Hoxc8) and phenotype independent (Adipoq) markers. Hierarchical clustering broadly grouped samples from each phenotype together, but was also able to differentiate between pre- and post-transplant samples (Fig 3D), indicating that the phenotype-specific expression profile was mostly, but not entirely conserved following transplant. Expression values for a representative selective gene for each phenotype are shown in Figure 3 E–G. Characteristic of the brown-selective genes, expression of UCP1 is maintained in brown grafts with transplant (Fig 3E) with no significant effect of transplant noted by 2-way ANOVA. However, characteristic of the beige-selective genes, expression of Tnfrsf9/CD137 is increased with transplant in all genotypes (Fig 3F) with a significant effect of transplant ($p<0.001$) and a significant transplant-phenotype interaction ($p<0.001$). White-selective Hoxc8 also exhibited a significant transplant-phenotype interaction ($p<0.001$) driven by increased expression in brown grafts and decreased expression in beige grafts with transplant. These findings are consistent with previous studies utilizing subcutaneous or visceral brown fat transplant that note modest changes in graft characteristics over time but an overall maintenance of phenotype-specific function and morphology[32; 33].

Transplanted brown fat increases adjacent muscle mass during regeneration

To explore the potential for phenotype-specific signals to influence muscle regeneration, intermuscular fat transplant was combined with cardiotoxin (CTX) injection into the graft-adjacent supraspinatus (SS) muscle. 14 days post-injection, regenerating SS muscles in the brown fat transplant group had ~10% more mass than beige, white or sham transplant groups (Fig 4A, effect size $\eta^2=0.30$). This effect was not seen with CTX injury to the graft-distant tibialis anterior (TA) muscle (Fig 4B), suggesting that it is driven by local rather than endocrine factors. Additionally, no difference in SS mass was seen in the absence of CTX in any transplant group (Fig 4C), suggesting that the signals are acting specifically on regenerative processes.

Increased muscle mass with brown fat transplant is associated with selective hypertrophy of superficial type IIb fibers during regeneration

Cellular changes in day 14 regenerating muscle were analyzed by immunohistochemistry in two regions – superficial (graft adjacent) and deep. Analysis of fiber cross-sectional areas subdivided by fiber type revealed a significant phenotype effect on type IIb fiber area in the superficial region (Fig 5 B, effect size $\eta^2=0.27$). Tukey post-testing revealed a significant increase in type IIb fiber areas with brown fat transplant compared with beige and sham transplant groups. No significant difference in fiber areas was detected in the deep regions of the muscles (Fig 5 C). There was also no significant effect of fat phenotype on fiber type of either region. In addition to fibers, two muscle resident cell populations known to influence regeneration were quantified – satellite cells and fibro/adipogenic progenitor (FAP) cells. No

effect of fat phenotype was found on the quantity of Pax7+ satellite cells or PDGFRα+ FAP cells in either superficial or deep regions of the muscles (Supplemental Figure 2).

Increased muscle mass with brown fat transplant is functional, leading to higher contractile force generation

To determine whether the increased mass of the brown graft-adjacent regenerating SS muscle conferred a functional benefit, ex-vivo contractile testing was performed at day 14 post-CTX. Peak tetanic force production in the SS was significantly higher with brown fat transplant than beige or sham transplant groups (Fig 6A, effect size η^2=0.42). When forces were normalized to PCSA, this difference was eliminated (Fig 6B) suggesting, with Figure 4, that brown fat transplant drives an increase in functional contractile material rather than an increase in normalized contractile capacity. Twitch contraction kinetics were not significantly different between groups, however there was a trend for both time to peak tension and half relaxation time to be shorter with brown fat transplant (Fig 6 C&D). This trend aligns with evidence for increased type IIb fiber area in this group (Fig 5B).

Discussion

A number of studies have hypothesized local cross-talk between muscle and adipose tissue[4–6]. Given the physical juxtaposition of the two tissues, it makes intuitive sense that secreted adipokines would locally affect muscle either through direct contact between adipocytes and muscle cells or via a shared microvasculature[5]. Because of the confounding effects of systemic disease and the non-invasive nature of human-based studies, this is not possible to demonstrate conclusively in humans. Recently, Liu et al. genetically ablated IMAT in muscle, demonstrating deficits in muscle regeneration that are presumably due to removal of “pro-myogenic” paracrine signals[22]. However, this model is unable to differentiate whether the signals arise from the bi-potent FAPs or mature IMAT. Indeed, undifferentiated FAPs promote myoblast differentiation[34] and in-vivo regeneration via an IL-4/IL-13 signaling switch which inhibits adipogenesis[23]. Thus, we believe this report to be the first demonstration of local signaling from mature adipose tissue to muscle.

To date, no models allow for the study of the local impact of mature fat on muscle physiology. Here we have developed a functional model of fat transplant to probe the features of adipose-muscle cross-talk. In this model, transplanted fat engrafts in the intermuscular space on the superficial surface of the SS muscle and is vascularized with no gross signs of rejection. Vascularization of the graft is likely driven by severed vessels in the graft becoming contiguous with the superficial vessels of the SS muscle on which the graft rests (visible in Fig 2 A&C). Thus, secreted cytokines could reach the muscle through a shared microvasculature or directly through the physical interface. Based on extensive evidence for endocrine action of adipokines on muscle[35] and the pro-regenerative action of a number of brown-fat specific adipokines[33; 36; 37], we hypothesize that mechanism underlies our effect. However, we are not able to rule out non-cytokine signaling as a mediator. Excess heat generated by the transplanted brown fat[38] or a unique immune profile[39] could also impact regeneration. Future work will explicitly test these potential mechanisms, however,

the data that we present in this work shows that graft-derived signals can indeed reach the muscle and exert a localized effect.

Because the signals arise from exogenous fat, this model allows isolation of graft characteristics (e.g. phenotype, disease state, age, genetic composition) from the systemic environment of the host. This is a powerful framework for mechanistically examining specific features of adipose signaling. This approach is not novel but rather has been used successfully with subcutaneous and visceral fat transplant of brown[32; 33], beige[28; 40] and white[41] fat depots to define depot-specific features of adipose endocrine signaling. We designed our model to transplant a relatively small fat mass (about 10% of previous models) to minimize endocrine effects and explore paracrine signaling. We do indeed see changes in regeneration in graft-adjacent muscle that are not observed in graft-distant muscle, however we did not comprehensively analyze the state of the muscles and thus cannot exclude graft-induced endocrine effects on other physiological processes.

Using this model, we have demonstrated that brown fat can promote muscle growth during regeneration. Absence of an effect with similar sized beige and white fat grafts indicates that the effect is phenotype-specific and not a general result of the transplant procedure. We did not observe any migration of graft-derived cells into the muscle belly, suggesting that indirect signaling likely underlies the anabolic effect of brown fat transplant. This work did not explore potential mediators of this effect. Brown fat secretes a number of adipokines involved in regeneration including IGF1[33], bFGF[36] and VEGF[37] which could act individually or in combination to increase regenerating muscle mass. Future work will examine candidate mediators with genetically modified graft donors. Because mouse models with visceral fat expansion exhibit impaired regeneration efficiency[42–44], we were surprised to find that visceral (white) fat transplant did not affect regeneration. However, pathological changes to visceral fat in these models of obesity may drive the secretion of harmful cytokines that are not seen in our lean donor animals. Similarly, we were surprised to find no beneficial effect of beige fat transplant. However, we hypothesize that beige fat may require stimulation to elicit pro-regenerative signaling. Future work will also explore the effect of obesity and stimulation in this model.

The data presented here are a snapshot of the muscle at a late stage of regeneration - complete regeneration takes about 4 weeks. At day 14 post-CTX injection, most provisional matrix and inflammatory cells have been replaced with regenerated fibers that are functional, though immature[29]. At this stage, muscle mass has returned to control levels, but a deficit in force production remains. We hypothesize that this deficit is due to incomplete fusion of type IIb fibers which were frequently found to be split with the appearance of a primary and secondary fiber within an endomysial boundary, an effect which has been reported previously in regenerating muscle[45]. As these split fibers ultimately resolve during later stages of regeneration ultimately resulting in increased muscle mass and contractile force[46], we hypothesize that our results with brown fat transplant represent an acceleration of the regenerative process. This could be due to increased efficiency of progenitor cells, most probably satellite cells, early in the regenerative process or improved hypertrophy in nascent fibers later. Further, brown fat grafts may directly signal these cells or act on them indirectly through supporting cells such as FAPs or infiltrating macrophages. Though we detected no

change in satellite cells or FAPs at day 14, these cells exert most of their effects in the first few days of regeneration and thus their numbers at later stages may not reflect their contribution at earlier stages. The work presented here was performed at day 14 to determine whether fat transplant would elicit a sustained response in regenerating muscle and now ongoing studies are defining the timeframe of cellular changes and whether tissue changes are retained after regeneration is complete.

Though CTX is a gold standard for studying muscle regeneration in mice[29], it is not representative of the loading signals for growth and regeneration that a human muscle is likely to experience. We chose CTX in this study because its cellular effects are dramatic and well-defined in mice, allowing us to better discern effects on fiber regeneration and growth. Frequently, excessive EMAT and IMAT accumulation are accompanied by signs of advanced muscle degeneration with disrupted fiber structure, necrosis and phagocytosis[47; 48]. Rehabilitation in this context is likely to require additional sources of contractile material, specifically regenerated fibers. While increased loading may initiate a modest regenerative or hypertrophic response, evidence for reduced sensitivity of IMAT infiltrated muscle to rehabilitation[12; 14] suggests that these alone are insufficient to restore function. We believe that a fuller understanding of the response of regenerating muscle to paracrine adipokines will assist in the development of adjuvant fat-targeted therapies that promote muscle regeneration and improve rehabilitative outcomes. Our work here suggests that adipokines derived from brown adipose tissue, so-called “batokines”, may promote muscle growth during regeneration. Though adult humans possess little classical brown fat, our work and that of others suggests that EMAT and IMAT can be stimulated to a more brown-like state[24; 25]. Whether browned EMAT or IMAT would replicate the paracrine signature of brown fat is unknown. However, mounting evidence suggests endocrine signaling overlap between brown and browned beige fat. Like transplant of brown fat, transplant of browned, but not naïve, beige fat improves muscle insulin sensitivity[28; 32]. Additionally, a genetic mouse model of fat browning exhibits anabolic effects in bone[27], like those hypothesized for brown fat[49]. Thus, a next important step in this research will be to test whether browned beige fat can similarly promote muscle growth during regeneration through paracrine signaling.

This work has a number of important limitations that should be discussed. First, this fat transplant model creates an artificial fat-muscle interface that may not reflect some subtleties of endogenous interfaces. Second, we used depots of mouse fat that likely differ from human EMAT and IMAT. Significant transcriptional differences exist between species in a given depot of adipose tissue and within a species between depots classified as beige fat[50]. EMAT and IMAT may have differing features, both from each other and from mouse fat, that uniquely define their interaction with muscle. Finally, regeneration was elicited in a healthy muscle that does not represent the degenerative pathology that frequently accompanies EMAT/IMAT accumulation. Environmental pressures such as chronic inflammation, depletion of the satellite cell pool and excessive stiffening of the extracellular matrix environment may impede the pro-regenerative action of paracrine adipose signaling. Further studies will be required to determine the full translational potential of the findings presented here.

In conclusion, we report the development of a novel intermuscular fat transplant model to study local signaling between adipose tissue and muscle. We demonstrate local signaling between muscle and adjacent adipose grafts and show that it is phenotype-specific where brown, but not beige or white, grafts promote muscle growth during regeneration. This finding points to adipose phenotype as novel player in muscle injury and disease pathology and supports its potential as a therapeutic target.

Supplementary Material

Refer to Web version on PubMed Central for supplementary material.

Acknowledgements

This work was supported by NIH 5P30AR057235–09.

References

1. de Jong JM, Larsson O, Cannon B, et al. 2015 A stringent validation of mouse adipose tissue identity markers. Am J Physiol Endocrinol Metab 308:E1085–1105. [PubMed: 25898951]
2. Eringa EC, Bakker W, van Hinsbergh VW. 2012 Paracrine regulation of vascular tone, inflammation and insulin sensitivity by perivascular adipose tissue. Vascul Pharmacol 56:204–209. [PubMed: 22366250]
3. Iacobellis G 2015 Local and systemic effects of the multifaceted epicardial adipose tissue depot. Nat Rev Endocrinol 11:363–371. [PubMed: 25850659]
4. Manini TM, Clark BC, Nalls MA, et al. 2007 Reduced physical activity increases intermuscular adipose tissue in healthy young adults. Am J Clin Nutr 85:377–384. [PubMed: 17284732]
5. Kelley DE, Goodpaster BH. 2015 Stewing in Not-So-Good Juices: Interactions of Skeletal Muscle With Adipose Secretions. Diabetes 64:3055–3057. [PubMed: 26294424]
6. Addison O, Marcus RL, Lastayo PC, et al. 2014 Intermuscular fat: a review of the consequences and causes. Int J Endocrinol 2014:309570. [PubMed: 24527032]
7. Marcus RL, Addison O, Kidde JP, et al. 2010 Skeletal muscle fat infiltration: impact of age, inactivity, and exercise. J Nutr Health Aging 14:362–366. [PubMed: 20424803]
8. Shen PH, Lien SB, Shen HC, et al. 2008 Long-term functional outcomes after repair of rotator cuff tears correlated with atrophy of the supraspinatus muscles on magnetic resonance images. J Shoulder Elbow Surg 17:1S–7S. [PubMed: 17931908]
9. Cheema B, Abas H, Smith B, et al. 2010 Investigation of skeletal muscle quantity and quality in end-stage renal disease. Nephrology (Carlton) 15:454–463. [PubMed: 20609098]
10. Delmonico MJ, Harris TB, Visser M, et al. 2009 Longitudinal study of muscle strength, quality, and adipose tissue infiltration. Am J Clin Nutr 90:1579–1585. [PubMed: 19864405]
11. Maly MR, Calder KM, Macintyre NJ, et al. 2013 Relationship of intermuscular fat volume in the thigh with knee extensor strength and physical performance in women at risk of or with knee osteoarthritis. Arthritis Care Res (Hoboken) 65:44–52. [PubMed: 23044710]
12. Marcus RL, Addison O, LaStayo PC. 2013 Intramuscular adipose tissue attenuates gains in muscle quality in older adults at high risk for falling. A brief report. J Nutr Health Aging 17:215–218. [PubMed: 23459972]
13. Bittel DC, Bittel AJ, Tuttle LJ, et al. 2015 Adipose tissue content, muscle performance and physical function in obese adults with type 2 diabetes mellitus and peripheral neuropathy. J Diabetes Complications 29:250–257. [PubMed: 25547717]
14. Gladstone JN, Bishop JY, Lo IK, et al. 2007 Fatty infiltration and atrophy of the rotator cuff do not improve after rotator cuff repair and correlate with poor functional outcome. Am J Sports Med 35:719–728. [PubMed: 17337727]

15. Gerber C, Schneeberger AG, Hoppeler H, et al. 2007 Correlation of atrophy and fatty infiltration on strength and integrity of rotator cuff repairs: a study in thirteen patients. J Shoulder Elbow Surg 16:691–696. [PubMed: 17931904]
16. Tuttle LJ, Sinacore DR, Mueller MJ. 2012 Intermuscular adipose tissue is muscle specific and associated with poor functional performance. J Aging Res 2012:172957. [PubMed: 22666591]
17. Hilton TN, Tuttle LJ, Bohnert KL, et al. 2008 Excessive adipose tissue infiltration in skeletal muscle in individuals with obesity, diabetes mellitus, and peripheral neuropathy: association with performance and function. Phys Ther 88:1336–1344. [PubMed: 18801853]
18. Marcus RL, Addison O, Dibble LE, et al. 2012 Intramuscular adipose tissue, sarcopenia, and mobility function in older individuals. J Aging Res 2012:629637. [PubMed: 22500231]
19. Buford TW, Lott DJ, Marzetti E, et al. 2012 Age-related differences in lower extremity tissue compartments and associations with physical function in older adults. Exp Gerontol 47:38–44. [PubMed: 22015325]
20. Torriani M, Townsend E, Thomas BJ, et al. 2012 Lower leg muscle involvement in Duchenne muscular dystrophy: an MR imaging and spectroscopy study. Skeletal Radiol 41:437–445. [PubMed: 21800026]
21. Freda PU, Shen W, Heymsfield SB, et al. 2008 Lower visceral and subcutaneous but higher intermuscular adipose tissue depots in patients with growth hormone and insulin-like growth factor I excess due to acromegaly. J Clin Endocrinol Metab 93:2334–2343. [PubMed: 18349062]
22. Liu W, Liu Y, Lai X, et al. 2012 Intramuscular adipose is derived from a non-Pax3 lineage and required for efficient regeneration of skeletal muscles. Dev Biol 361:27–38. [PubMed: 22037676]
23. Heredia JE, Mukundan L, Chen FM, et al. 2013 Type 2 innate signals stimulate fibro/adipogenic progenitors to facilitate muscle regeneration. Cell 153:376–388. [PubMed: 23582327]
24. Meyer GA, Gibbons MC, Sato E, et al. 2015 Epimuscular Fat in the Human Rotator Cuff Is a Novel Beige Depot. Stem Cells Transl Med 4:764–774. [PubMed: 25999520]
25. Crisan M, Casteilla L, Lehr L, et al. 2008 A reservoir of brown adipocyte progenitors in human skeletal muscle. Stem Cells 26:2425–2433. [PubMed: 18617684]
26. Laurens C, Louche K, Sengenes C, et al. 2016 Adipogenic progenitors from obese human skeletal muscle give rise to functional white adipocytes that contribute to insulin resistance. Int J Obes (Lond) 40:497–506. [PubMed: 26395744]
27. Rahman S, Lu Y, Czernik PJ, et al. 2013 Inducible brown adipose tissue, or beige fat, is anabolic for the skeleton. Endocrinology 154:2687–2701. [PubMed: 23696565]
28. Stanford KI, Middelbeek RJ, Townsend KL, et al. 2015 A novel role for subcutaneous adipose tissue in exercise-induced improvements in glucose homeostasis. Diabetes 64:2002–2014. [PubMed: 25605808]
29. Hardy D, Besnard A, Latil M, et al. 2016 Comparative Study of Injury Models for Studying Muscle Regeneration in Mice. PLoS One 11:e0147198. [PubMed: 26807982]
30. Meyer GA. 2018 Evidence of induced muscle regeneration persists for years in the mouse. Muscle Nerve 58:858–862. [PubMed: 30159908]
31. Wu J, Boström P, Sparks LM, et al. 2012 Beige adipocytes are a distinct type of thermogenic fat cell in mouse and human. Cell 150:366–376. [PubMed: 22796012]
32. Stanford KI, Middelbeek RJ, Townsend KL, et al. 2013 Brown adipose tissue regulates glucose homeostasis and insulin sensitivity. J Clin Invest 123:215–223. [PubMed: 23221344]
33. Gunawardana SC, Piston DW. 2012 Reversal of type 1 diabetes in mice by brown adipose tissue transplant. Diabetes 61:674–682. [PubMed: 22315305]
34. Joe AW, Yi L, Natarajan A, et al. 2010 Muscle injury activates resident fibro/adipogenic progenitors that facilitate myogenesis. Nat Cell Biol 12:153–163. [PubMed: 20081841]
35. Trayhurn P, Drevon CA, Eckel J. 2011 Secreted proteins from adipose tissue and skeletal muscle - adipokines, myokines and adipose/muscle cross-talk. Arch Physiol Biochem 117:47–56. [PubMed: 21158485]
36. Yamashita H, Sato N, Kizaki T, et al. 1995 Norepinephrine stimulates the expression of fibroblast growth factor 2 in rat brown adipocyte primary culture. Cell Growth Differ 6:1457–1462. [PubMed: 8562484]

37. Fredriksson JM, Lindquist JM, Bronnikov GE, et al. 2000 Norepinephrine induces vascular endothelial growth factor gene expression in brown adipocytes through a beta -adrenoreceptor/cAMP/protein kinase A pathway involving Src but independently of Erk½. J Biol Chem 275:13802–13811. [PubMed: 10788502]
38. Kojima A, Goto K, Morioka S, et al. 2007 Heat stress facilitates the regeneration of injured skeletal muscle in rats. J Orthop Sci 12:74–82. [PubMed: 17260121]
39. Qiu Y, Nguyen KD, Odegaard JI, et al. 2014 Eosinophils and type 2 cytokine signaling in macrophages orchestrate development of functional beige fat. Cell 157:1292–1308. [PubMed: 24906148]
40. Tran TT, Yamamoto Y, Gesta S, et al. 2008 Beneficial effects of subcutaneous fat transplantation on metabolism. Cell Metab 7:410–420. [PubMed: 18460332]
41. Gavrilova O, Marcus-Samuels B, Graham D, et al. 2000 Surgical implantation of adipose tissue reverses diabetes in lipoatrophic mice. J Clin Invest 105:271–278. [PubMed: 10675352]
42. Nguyen MH, Cheng M, Koh TJ. 2011 Impaired muscle regeneration in ob/ob and db/db mice. ScientificWorldJournal 11:1525–1535. [PubMed: 21805021]
43. Vignaud A, Ramond F, Hourdé C, et al. 2007 Diabetes provides an unfavorable environment for muscle mass and function after muscle injury in mice. Pathobiology 74:291–300. [PubMed: 17890896]
44. Fu X, Zhu M, Zhang S, et al. 2016 Obesity Impairs Skeletal Muscle Regeneration Through Inhibition of AMPK. Diabetes 65:188–200. [PubMed: 26384382]
45. Karalaki M, Fili S, Philippou A, et al. 2009 Muscle regeneration: cellular and molecular events. In Vivo 23:779–796. [PubMed: 19779115]
46. Vignaud A, Hourdé C, Butler-Browne G, et al. 2007 Differential recovery of neuromuscular function after nerve/muscle injury induced by crude venom from Notechis scutatus, cardiotoxin from Naja atra and bupivacaine treatments in mice. Neurosci Res 58:317–323. [PubMed: 17485127]
47. Gibbons MC, Singh A, Anakwenze O, et al. 2017 Histological Evidence of Muscle Degeneration in Advanced Human Rotator Cuff Disease. J Bone Joint Surg Am 99:190–199. [PubMed: 28145949]
48. Drachman DB, Murphy SR, Nigam MP, et al. 1967 “Myopathic” changes in chronically denervated muscle. Arch Neurol 16:14–24. [PubMed: 6024250]
49. Motyl KJ, Rosen CJ. 2011 Temperatures rising: brown fat and bone. Discov Med 11:179–185. [PubMed: 21447277]
50. Komolka K, Albrecht E, Wimmers K, et al. 2014 Molecular heterogeneities of adipose depots - potential effects on adipose-muscle cross-talk in humans, mice and farm animals. J Genomics 2:31–44. [PubMed: 25057322]

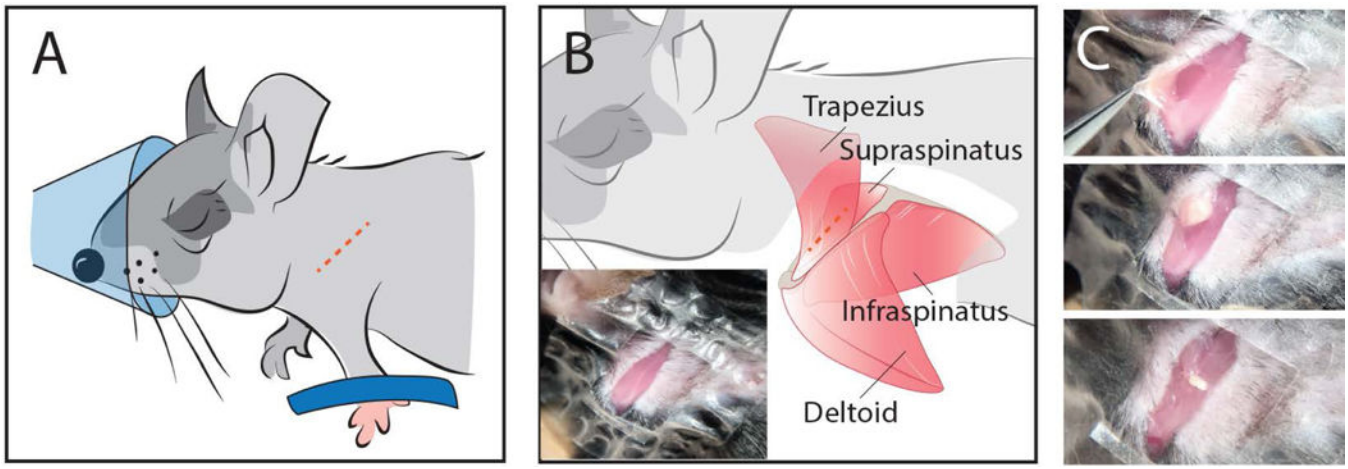

Figure 1.

Illustration of fat transplant procedure. (A) Schematic location of skin incision (dotted line) over the scapular spine. (B) Schematic location of muscular incision through the trapezius muscle (dotted line). Inset shows the exposed musculature in a mouse. (C) Generation of an intermuscular pocket (top) for insertion of fat explants (middle) followed by closure of the pocket with suture (bottom).

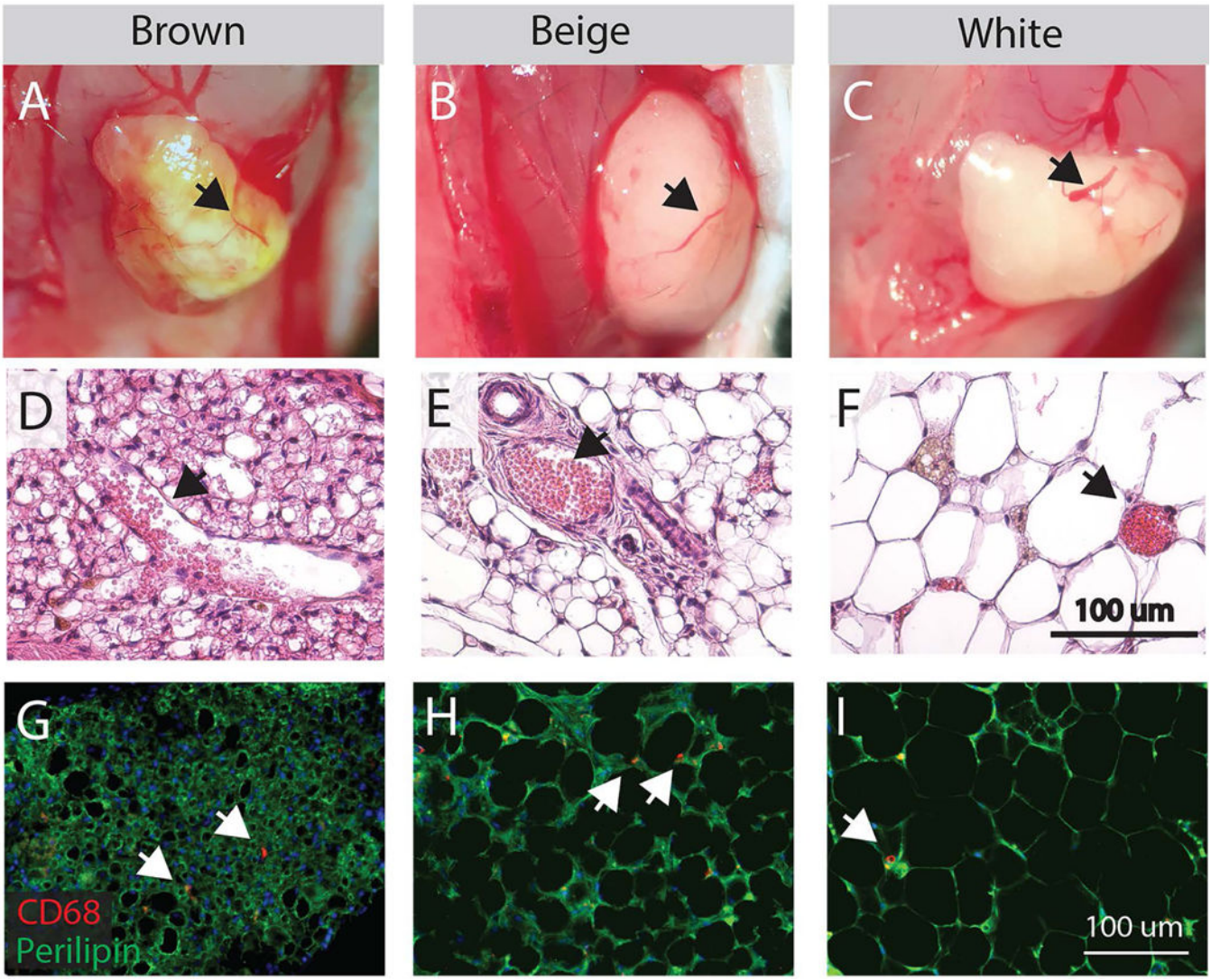

Figure 2.

Characterization of transplanted fat engraftment. (A-C) Gross images of fat 14 days post-transplant on the surface of the supraspinatus muscle following removal of the overlying trapezius muscle. Brown, beige and white grafts have visible red vessels that bleed when cut (arrows). (D-F) Vessels identified on H&E stained sections of fat grafts (arrows) contain red blood cells (pink circles). Adipocytes in brown and beige fat exhibit multilocular morphology (multiple lipid droplets per cell). (G-I) CD68 staining for macrophages in fat grafts reveals a diffuse distribution of positive cells (arrows) amongst perilipin positive adipocytes.

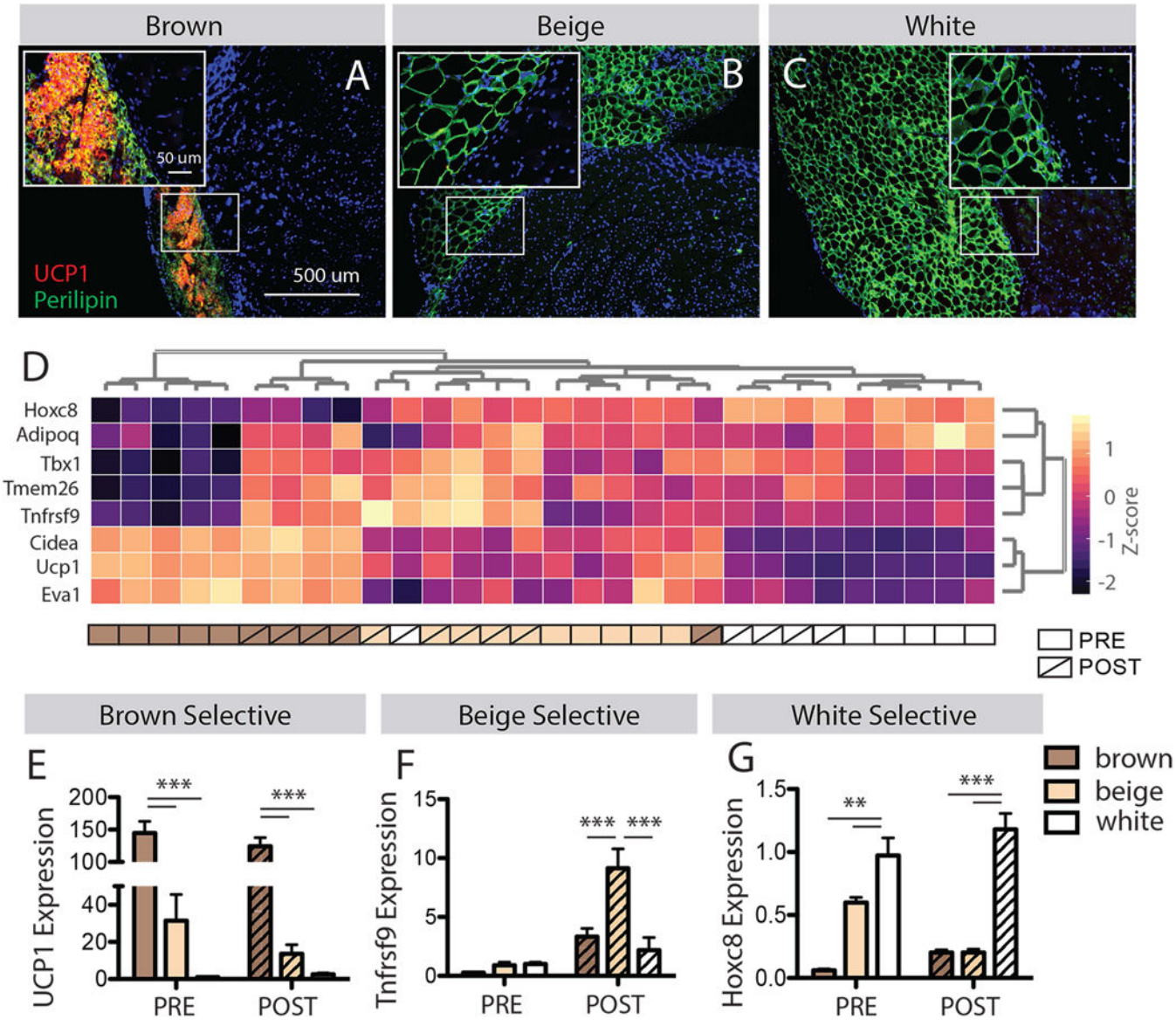

Figure 3.

Characterization of transplanted fat phenotype. (A-C) Histological sections of the graft-muscle interface stained for the brown fat selective marker UCP1. Insets show a tight junction between brown, beige and white grafts (perilipin positive adipocytes) and muscle (adjacent DAPI positive nuclei). Only brown grafts have detectable UCP1 by immunostaining. (D) Hierarchical clustering of fat samples pre- and 14 days post-transplant by expression of 8 phenotype selective genes. Expression of these genes effectively separates brown, beige and white fats pre-transplant and clusters most post-transplant samples with their pre-transplant phenotype. (E-G) Expression of representative brown, beige and white fat selective genes from the panel in D by fat phenotype and transplant state. ** $p<0.01$, *** $p<0.005$.

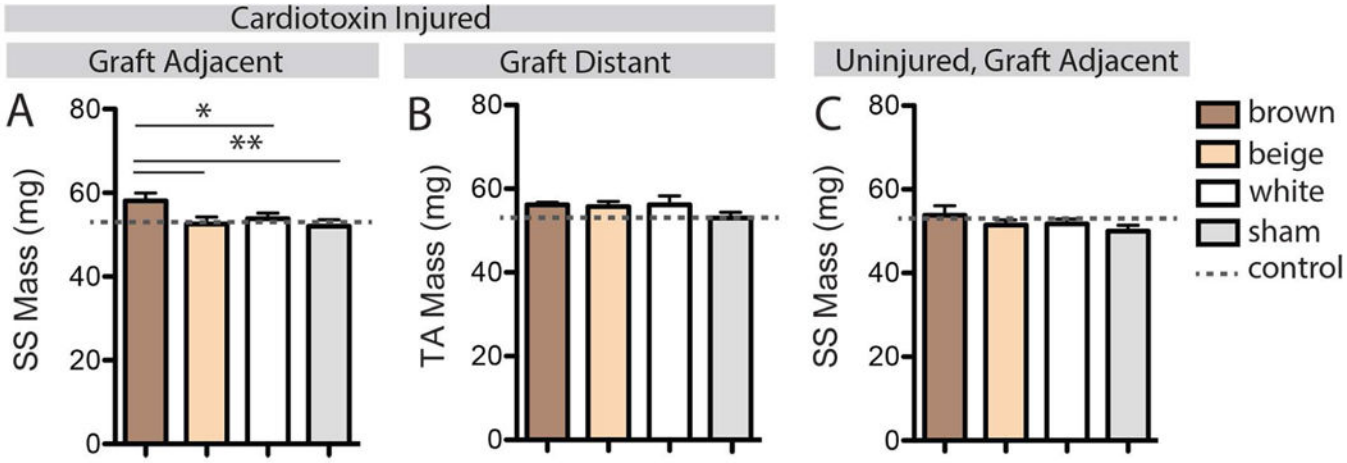

Figure 4.

Measurements of muscle mass with combinations of fat transplant and injury. (A) The mass of the graft-adjacent cardiotoxin injured SS muscle was significantly increased in the brown fat transplant group. (B) No effect of fat transplant was found in the anatomically distant cardiotoxin injured TA muscle. (C) No effect of fat transplant was found in adjacent uninjured (saline injected) SS muscles. * $p<0.05$, ** $p<0.01$.

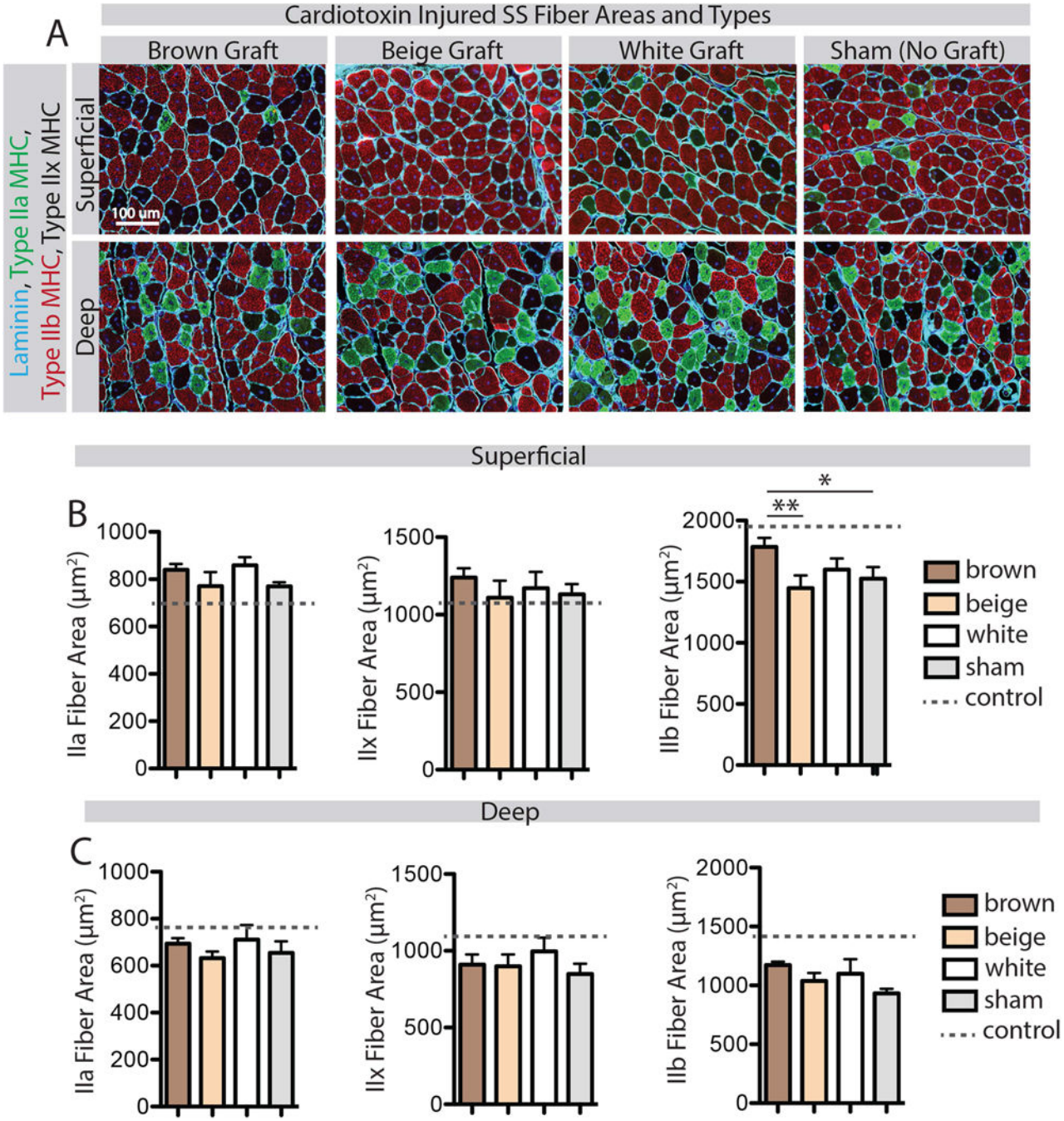

Figure 5.

Analysis of fiber cross-sectional areas by fiber type. (A) Representative images of superficial (graft-adjacent) and deep regions of CTX-injured SS muscles in the four transplant groups stained for type IIa and IIb myosin heavy chain (MHC) and counterstained with laminin to indicate fiber boundaries. Unstained fibers were confirmed on sequentially stained sections to all be positive for type IIx MHC. (B) Quantification of cross-sectional areas of type IIa, IIx and IIb fibers in the superficial region. The brown fat transplant group had increased type IIb fiber areas only, compared with beige and sham transplant groups. (C) Quantification of

cross-sectional areas of type IIa, IIx and IIb fibers in the deep region. There was no effect of fat transplant on any fiber type in this region. * $p<0.05$, ** $p<0.01$.

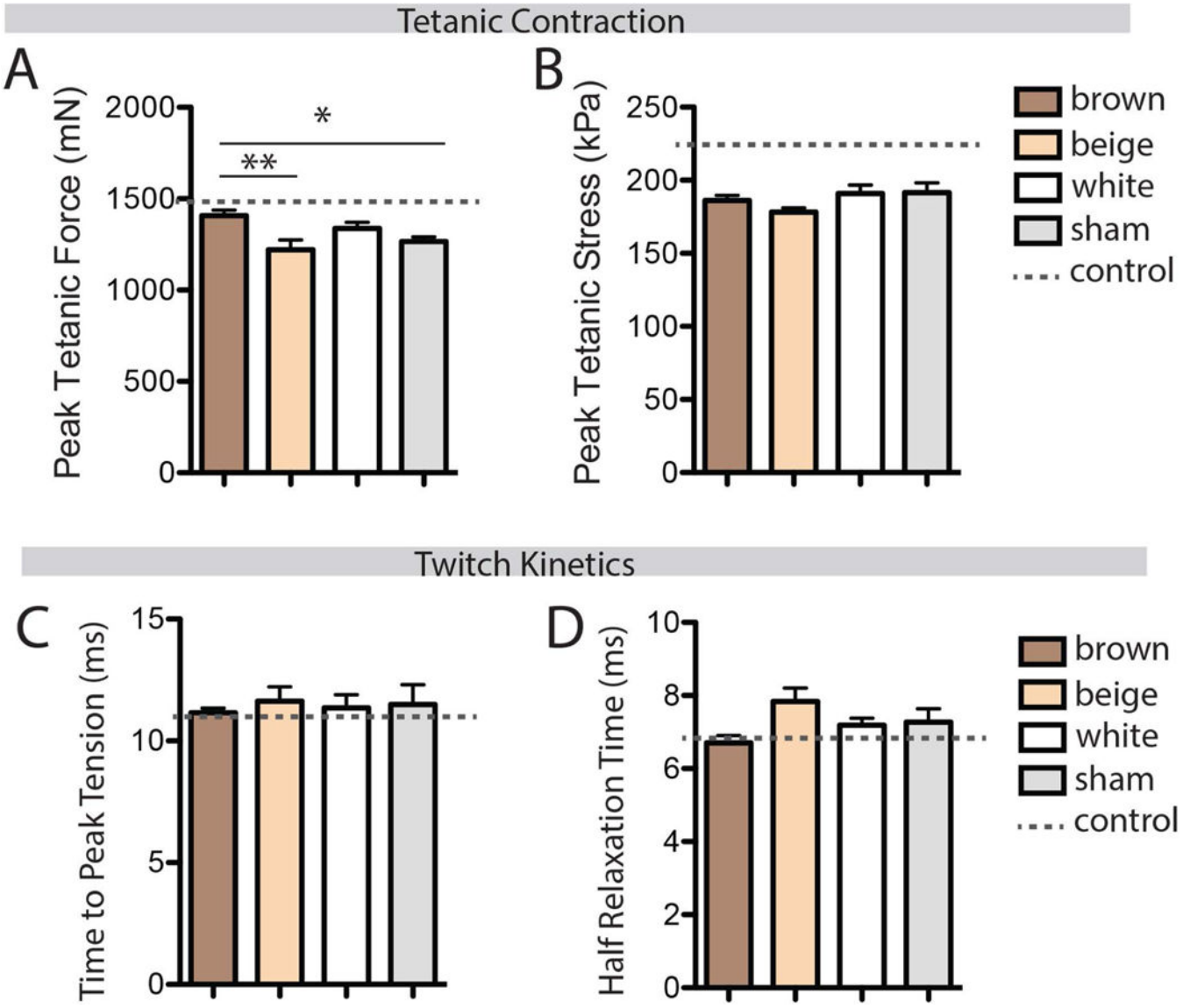

Figure 6.

Assessment of muscle contractile function with ex-vivo stimulation. (A) Peak tetanic force was elevated in the brown fat transplant group compared with beige and sham transplants. (B) No effect of fat transplant was found in peak tetanic stress (peak tetanic force normalized to muscle physiological cross-sectional area). (C-D) No effect of fat transplant was found in either time to peak tension or half relaxation time, two measures of twitch kinetics. * $p<0.05$, ** $p<0.01$.